



Research Article

NUMERICAL HEAT TRANSFER STUDY IN A ROUND TUBE WITH INCLINED RECTANGULAR RINGS

N. Koolnapadol¹
S. Sripattanapipat^{2,*}
S. Skullong³
P. Wiriyavitsajjar⁴
W. Thungwinyoo⁴
C. Suppasubsiri⁴

¹ Department of Automotive Mechanical Engineering, Faculty of Industrial Technology, Rajabhat Rajanagarindra University, Chachoengsao 24000, Thailand

² Mechanical Engineering Dept., Faculty of Engineering, Mahanakorn University of Technology, Bangkok, 10530, Thailand

³ Energy Systems Research Group, Department of Mechanical Engineering, Faculty of Engineering at Sriracha, Kasetsart University Sriracha Campus, Chonburi 20230, Thailand

⁴ Department of Mechanical Engineering, Faculty of Engineering, King Mongkut's Institute of Technology Ladkrabang, Bangkok 10520, Thailand

ABSTRACT:

This paper deals with a numerical study on heat transfer and flow characteristics in a round tube inserted with inclined rectangular rings (IRR). The IRR elements at attack angle of 45° were mounted periodically into the test tube. Air was employed as the test fluid with Reynolds number from 3,000 to 18,000. The study reveals that the insertion of IRR elements can create two counter-rotating vortices along the tube that help increase the turbulence intensity apart from conveying the colder fluid from the core region to the heated-wall region. The IRR insert provides the high heat transfer and pressure drop increase than the smooth tube alone. Also, the tube fitted with IRR has considerably higher thermal performance than the smooth tube. The highest thermal performance for using the 45° IRR is found to be 2.12 at BR=0.2 and PR=0.5.

Keywords: Numerical analysis; Heat transfer; Vortex ring; Turbulent flow

1. INTRODUCTION

Many techniques for improving the heat transfer rate in a heat exchanger system are needed to obtain much higher thermal performance of such a system leading to energy and cost saving. These techniques can be divided into two main groups. One is the active method which require external power sources while the other is the passive method which requires no power for the system such as surface coating, extended surface, ribbed tubes and various tube inserts. In general, the latter is more popular than the former, especially for insert devices.

For years, many researchers have paid attentions to find the ways to use the insert devices effectively. Ring inserts in tubes have been widely used in engineering applications. Kongkaietpaiboon et al. [1] studied the heat transfer augmentation by inserting circular rings into a round tube and reported that the heat transfer is up to 57% to 195% above the smooth tube alone.

* Corresponding author: S. Sripattanapipat
E-mail address: ssomchai@mut.ac.th



Promvonge et al. [2] investigated thermal behaviors in a tube fitted with 30° inclined rings and found that the use of inclined rings provides considerable higher thermal performance than the transverse or 90° rings due to lower pressure drop, at similar ring parameters and operating conditions. Promvonge et al. [3] again studied the effect of pitch ratios ($PR = 0.5, 1.0$ and 2) and blockage ratios ($BR = 0.1, 0.15$ and 0.2) of newly inclined horseshoe-baffles inserted in a round tube on its heat transfer enhancement and reported that the tube fitted with inclined horseshoe baffles provided significant enhancement of the heat transfer rate around $92\text{--}208\%$ over the smooth tube while the friction loss is increased at about $1.76\text{--}6.37$ times. Sheikholeslami et al. [4] carried out an experiment to find the effect of perforated circular ring on fluid flow friction and heat transfer augmentation in an air-to-water heat exchanger system and found that the opening area of the ring has the maximum sensitivity on thermal performance of the system. Experimental investigation on turbulent convection heat transfer in a heat exchanger tube with solid hollow circular disk inserts was introduced by Kumar et al. [5]. An experimentally and numerically analysis on turbulent flow friction and heat transfer in a double pipe air-to-water heat exchanger equipped with conical rings were reported by Sheikholeslami et al. [6]. They showed that the thermal performance increases with increase of the pitch ratio while it decreases with the increase in Reynolds number. Chingtuaythong et al. [7] conducted an experiment by inserting 30° V-shaped circular rings into a round tube and indicated that the V-shaped rings can improve the heat transfer and friction factor.

For numerical work on ring inserts, Akansu [8] carried out a numerical analysis on the influence of space or pitch between porous rings and demonstrated that the heat transfer rate and friction factor increase with decreasing ring spacing. Similarly, Ozceyhan et al. [9] performed numerically to examine the effect of space/gap between the circular ring and tube wall on heat transfer rate and friction factor and showed that the rings should not be attached to the tube wall, to achieve higher thermal performance. Promvonge et al. [10] numerically investigated the heat transfer characteristics in a tube fitted with angled rings using Al_2O_3 water nanofluid and found that the performance was increased twice for using both the ring and the nanofluid together. Sripattanapipat et al. [11] performed a numerical study for turbulence heat transfer and flow structure in a heat exchanger tube fitted with V-shaped hexagonal conical rings (V-HCR) inserts and suggested that the V-HCR yielded considerably higher thermal performance than the typical conical ring.

In the literature review above, it is seen that the tube with inclined rings provides higher heat transfer and thermal performance than the one with vertical rings. Those works triggered the present work by modifying the inclined round ring to be the other shape rather than inclined circular rings. Therefore, the use of inclined rectangular rings (IRR) is proposed in the current work by inserting the IRR elements into an isothermal-fluxed tube at attack angle of 45° . The present work aims at studying the heat transfer and flow characteristics in a circular tube fitted with 45° inclined rectangular rings using a CFD (Computational Fluid Dynamics) simulation. The numerical computations for a three dimensional turbulent periodic flow through 45° IRR placed repeatedly in the tube are conducted for Reynolds number (Re) ranging from 3000 to $18,000$.

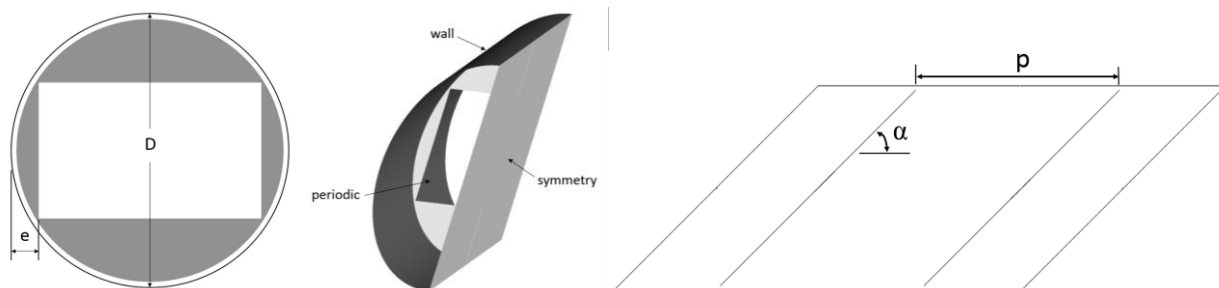


Fig. 1. Tube geometry and computational domain.

2. TUBE FLOW CONFIGURATION

The tube flow model in the current work is characterized by 45° inclined rectangular rings inserted repeatedly into a circular tube as shown in Fig. 1. The tube flow model under consideration is expected to attain a periodically fully developed flow where the velocity field repeats itself from one module to another. In this flow model, the air flows into the ring-inserted tube having the inner diameter, $D=20$ mm at inlet temperature, $T_{in}=300$ K. The geometrical ring

parameters, apart from a single attack angle (α) of 45° , include e and P that are, respectively, ring-width measured from tube surface to inner ring as shown in Fig. 1 and axial pitch distance between two adjacent rings. The ratio of ring width to tube diameter called the blockage ratio, $BR=e/D$, and the ratio of ring pitch to tube diameter called pitch ratio, $PR=P/D$, are varied in the range of 0.1 to 0.2 and 0.5 to 2.0, respectively.

3. COMPUTATIONAL DETAILS

3.1 Governing equations

The governing equations are the three-dimensional incompressible steady-state Reynolds-averaged Navier-Stokes (RANS) equations and the energy equation.

Continuity equation:

$$\frac{\partial}{\partial x_i}(\rho u_i) = 0 \quad (1)$$

Momentum equation:

$$\frac{\partial}{\partial x_j}(\rho u_i u_j) = -\frac{\partial p}{\partial x_i} + \frac{\partial}{\partial x_j} \left[\mu \left(\frac{\partial u_i}{\partial x_j} - \rho \overline{u'_i u'_j} \right) \right] \quad (2)$$

where ρ is fluid density, u_i is mean velocity component in direction x_i , p is pressure, μ is dynamic viscosity, and u' is a fluctuating velocity component. Repeated indices indicate summation from one to three for 3D problems.

Energy equation:

$$\frac{\partial}{\partial x_i}(\rho u_i T) = \frac{\partial}{\partial x_j} \left((\Gamma + \Gamma_t) \frac{\partial T}{\partial x_j} \right) \quad (3)$$

in which Γ and Γ_t are molecular thermal diffusivity and turbulent thermal diffusivity, respectively and are given by

$$\Gamma = \frac{\mu}{Pr}, \text{ and } \Gamma_t = \frac{\mu_t}{Pr_t} \quad (4)$$

The Realizable k - ϵ turbulence model was employed for closure of the Reynolds stress terms in Eq. (2). In the Realizable k - ϵ turbulence model, the Boussinesq hypothesis was used for modeling the Reynolds stress terms. The QUICK numerical scheme was employed for discretizing all the governing equations. The computation was based on the finite volume approach and the SIMPLE algorithm was used for handling the pressure-velocity coupling. No slip and constant temperature were set for boundary conditions of tube wall while adiabatic surface was utilized for the ring. The fully-developed periodic flow condition was applied to the inlet and outlet sections while due to plane symmetry of the tube, only half of the tube section module was used as computational domain as shown in Fig. 1. The solutions were converged when the residual values were less than 10^{-6} for all variables but less than 10^{-9} only for the energy equation.

There are four parameters of interest included Reynolds number (Re), friction factor (f), Nusselt number (Nu) and thermal enhancement factor (TEF). The Re is defined as

$$Re = \frac{\rho \bar{u} D}{\mu} \quad (5)$$

The f is evaluated from pressure drop, Δp across the tube length, P as

$$f = \frac{(\Delta p / P)D}{(1/2)\rho\bar{u}^2} \quad (6)$$

The local Nu is calculated by

$$Nu_x = \frac{h_x D}{\lambda} \quad (7)$$

where λ is fluid thermal conductivity.

The area-averaged Nu is obtained from

$$Nu = \frac{1}{A} \int Nu_x \partial A \quad (8)$$

The thermal enhancement factor (TEF) defined as the ratio of the dimensionless heat transfer coefficient of the ribbed tube, Nu to that of the smooth tube, Nu_0 , at an equal pumping power is given by

$$TEF = \frac{Nu / Nu_0}{(f / f_0)^{1/3}} \quad (9)$$

in which Nu_0 and f_0 are Nusselt number and friction factor for the smooth tube, respectively.

4. RESULTS AND DISCUSSION

4.1 Grid independence

Four sets of grids with different sizes were used for the simulation to ensure that the results were grid independence solutions. The average Nusselt number and friction factor for the four sets of grids at Reynolds number of 5000 are listed in Table 1. In the table, the relative difference of the simulation results between a grid of 193710 elements and 406796 elements was 0.85% for Nusselt number and 0.01% for friction factor. Therefore, the grid was considered to be sufficiently fine for use in the simulation at $Re=5000$. The grid system of about 200,000 elements was used for the current simulation.

Table 1: Grid independence test for $Re = 5000$

Grid size	Nu	f
52711	56.3164	0.25201
95991	55.4847	0.25035
193710	54.6714	0.24949
406796	54.2080	0.24948

4.2 Validation

The comparison between numerical and experimental results of Nu and f of a round tube with 30° inclined circular ring insert at BR=0.1, PR=1.0 as taken from [2] is depicted in Fig. 2(a) and 2(b), respectively. In the figure, the numerical results are found to be in good agreement with experimental data [2] for both Nu and f . The errors are within $\pm 12\%$ for Nu and $\pm 6\%$ for f . Therefore, the numerical flow model used in the current study can be considered to be reliable.

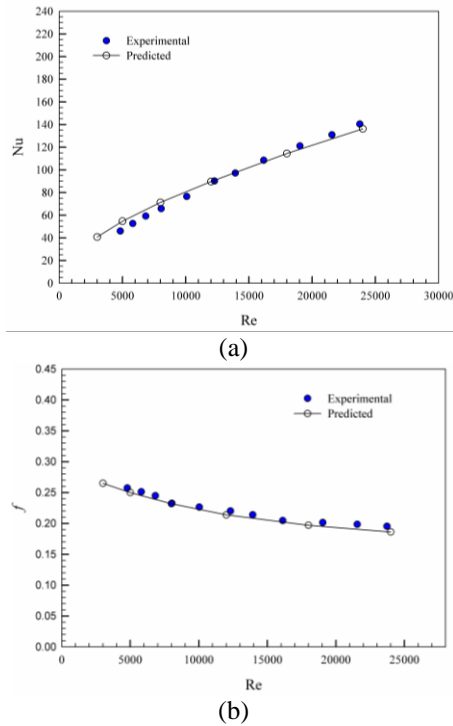


Fig. 2. Validation of numerical (a) Nu and (b) f with measurements of 30° inclined circular ring [2], BR=0.1, PR=1.0.

4.3 Flow structure and heat transfer

Figure 3(a) and (b) depicts streamlines and temperature contours in transverse planes at various locations for the IRR at BR=0.1, PR=1.0 and Re=8000, respectively. As seen in the figure, the IRR can generate two main vortices. A closer look reveals that the existence of IRR causes two main counter-rotating vortices that become common-flow-down vortices to the bottom wall. Thus, these counter-rotating vortices are responsible for the heat transfer augmentation in the tube, especially at the lower part area of the tube since those vortices give rise to vortex-induced impingement of flow (or VI effect). In Fig. 3(b), it is visible that the fluid temperature from the core is induced to the near-wall region due to the presence of the IRR. The low temperature area can be observed near the bottom wall regime while the high one can be seen in the top region.

Figure 4 exhibits local surface Nu contours for using IRR with BR=0.1, PR=1.0 at Re=8,000. It is seen that the higher Nusselt number area appears on the bottom wall region close to the ring while the lower Nu region is found on the upper tube, as expected. The peak area (in red area) is found in the tube wall region below the ring.

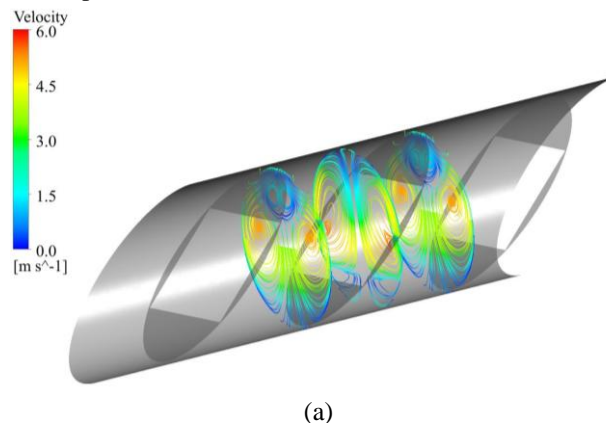


Fig. 3. (a) Streamlines and (b) temperature contours in transverse planes for IRR insert at BR=0.1, PR=1.0 and Re=8000.

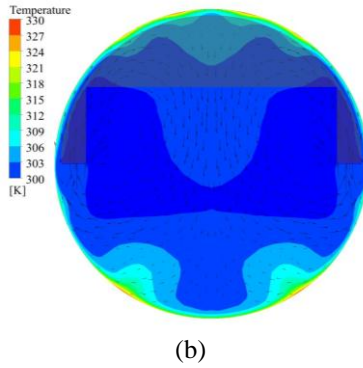


Fig. 3. (a) Streamlines and (b) temperature contours in transverse planes for IRR insert at BR=0.1, PR=1.0 and Re=8000 (Continued).

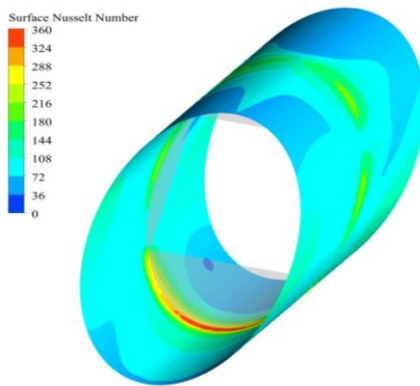


Fig. 4. Local Nu_x contours on tube wall for IRR insert at BR=1.0, PR=0.1, Re=8000.

4.4 Heat transfer result

Figure 5 displays the variation of Nu/Nu_0 with Re for IRR insert at different BR and PR values. The figure shows that Nu/Nu_0 tends to decrease with increasing Re. The Nu/Nu_0 also has the downtrend with increasing BR and PR for the IRR insert. The maximum Nu/Nu_0 is about 7.11 at Re = 3000, BR = 0.2 and PR = 0.5 while the minimum Nu/Nu_0 is around 2.8 at Re = 18,000, BR = 0.15 and PR = 2.0. The peak of Nu/Nu_0 is found for PR=0.5. This is because the use of the smaller PR can induce larger recirculation or vortex flow appearing behind the ring than that of the larger PR.

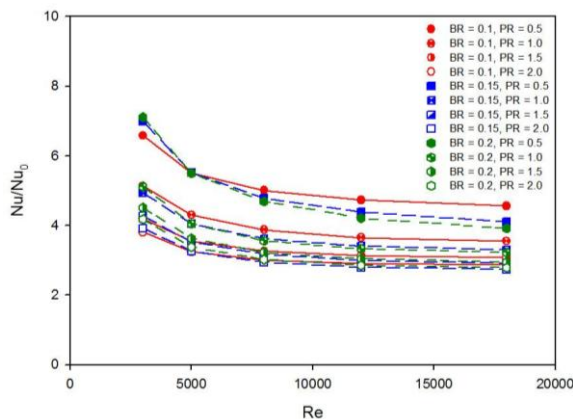


Fig. 5. Variation of Nu/Nu_0 with Re for IRR insert.

4.5 Friction loss result

The variation of f/f_0 with Re for using IRR insert with various BR and PR values is depicted in Fig. 6. In the figure, it is noted that f/f_0 tends to increase as Re increases. A close examination reveals that f/f_0 tends to decrease with increasing BR and PR values. This can be explained that higher BR can reduce the flow blockage areas on the lower and upper parts of the rings leading to lower the pressure drop increase. The highest f/f_0 is about 107 times at Re = 18,000, BR=0.1 and PR=0.5 while the lowest one is around 16 times at BR=0.2, PR=2.0 and Re=3000.

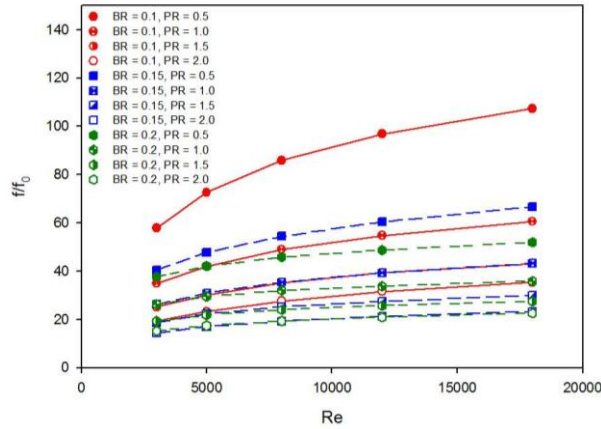


Fig. 6. Variation of f/f_0 with Re for IRR insert.

4.6 Thermal enhancement factor

Figure 7 portrays the distribution of TEF with Re for IRR inserts with different BR and PR values. It is visible that TEF tends to decrease steeply from the beginning with increasing Re until Re \approx 8000 and then reduce gradually for further Re. The maximum TEF of around 2.12 is at Re= 3000, BR=0.2 and PR=0.5 while the minimum one of about 0.9 is at Re = 18,000, BR = 0.1 and PR = 2.0. Thus, the use of IRR at lower BR (BR=0.1) and larger PR (PR=2.0) should be avoided due to lower TEF (TEF=1.0 is equal to smooth tube alone that means no advantage of heat gain from the insert).

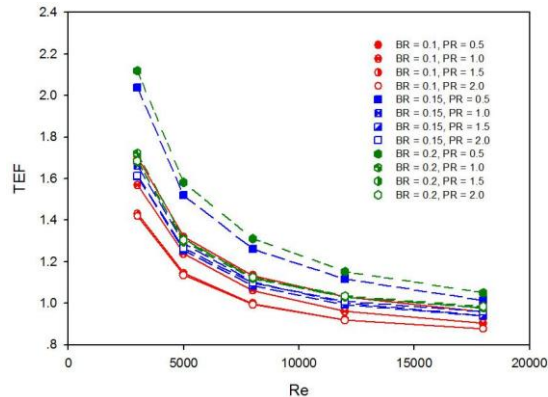


Fig. 7. Variation of TEF with Re for IRR insert.

5. CONCLUSIONS

A numerical study on turbulent airflow and heat transfer characteristics in an isothermal-fluxed tube fitted with IRR elements has been investigated. The simulation based on the finite volume method has been performed by using a fully developed periodic turbulent flow model. The use of IRR insert can generate two main counter-rotating vortices along the tube leading to considerable heat transfer augmentation. The heat transfer enhancement is about 2.74 to 7.11 times higher than the smooth tube alone and also the enlarged pressure loss in terms of friction factor is in the range of 14.3 to 107.4 times depending on BR, PR and Re values. The TEF of the inserted tube is above unity

only for $PR < 1.5$ and $BR > 0.1$ and has a maximum of about 2.12 at $Re = 3000$, $BR = 0.2$ and $PR = 0.5$. This indicates that the presence of the IRR elements can help increase heat transfer in the heat exchanger effectively. Thus, the IRR insert is considered to be one of the promising device for thermal performance improvement of a tubular heat exchanger.

NOMENCLATURE

A	convection heat transfer area, m^2
BR	blockage ratio (e/D)
D	inner diameter of tube, m
e	ring width, m
f	friction factor
h	convective heat transfer coefficient, $W/m^2 K$
k	turbulence kinetic energy
IRR	inclined rectangular ring
Nu	Nusselt number
P	axial pitch length of ring, m
p	static pressure, Pa
Pr	Prandtl number
PR	pitch ratio ($=P/D$)
Re	Reynolds number
T	temperature, K
TEF	thermal enhancement factor
u_i	velocity component in x_i -direction, m/s
\bar{u}	mean velocity, m/s

Greek letter

μ	dynamic viscosity, $kg/m s$
Γ	thermal diffusivity
λ	thermal conductivity of fluid, $W/m K$
α	attack angle, degree
ρ	fluid density, kg/m^3
ε	dissipation rate of turbulence kinetic energy, m^2/s^3

Subscripts

in	inlet
0	smooth tube
t	turbulent

REFERENCES

- [1] V. Kongkaitpaiboon, K. Nanan, S. Eiamsa-ard, Experimental investigation of convective heat transfer and pressure loss in a round tube fitted with circular-ring turbulators, *Int. Commun. Heat Mass Transf.*, Vol. 37, 2010, pp. 568–574.
- [2] P. Promvong, N. Koolnapadol, M. Pimsarn, C. Thianpong, Thermal performance enhancement in a heat exchanger tube fitted with inclined vortex rings, *Appl. Therm. Eng.*, Vol. 62, 2014, pp. 285-292.
- [3] P. Promvong, S. Tamna, M. Pimsarn, C. Thianpong, Thermal characterization in a circular tube fitted with inclined horseshoe baffles, *Appl. Therm. Eng.*, Vol. 75, 2015, pp. 1147–1155.
- [4] M. Sheikholeslami, M. Gorji-Bandpy, D.D. Ganji, Experimental study of the influence of perforated circular-ring on pressure loss and heat transfer enhancement using sensitivity analysis, *Appl. Therm. Eng.*, Vol. 91, 2015, pp. 739–748.
- [5] A. Kumar, S. Chamoli, M. Kumar, Experimental investigation on thermal performance and fluid flow characteristics in heat exchanger tube with solid hollow circular disk inserts, *Appl. Therm. Eng.*, Vol. 100, 2016, pp. 227–236.

- [6] M. Sheikholeslami, D.D. Ganji, M. Gorji-Bandpy, Experimental and numerical analysis for effects of using conical ring on turbulent flow and heat transfer in a double pipe air to water heat exchanger, *Appl. Therm. Eng.*, Vol. 100, 2016, pp. 805–819.
- [7] W. Chingtuaythong, P. Promvong, C. Thianpong, M. Pimsarn, Heat transfer characterization in a tubular heat exchanger with V-shaped rings, *Appl. Therm. Eng.*, Vol. 110, 2017, pp. 1164-1171.
- [8] S.O. Akansu, Heat transfers and pressure drops for porous-ring turbulators in a circular pipe, *Appl. Energy*, Vol. 83, 2006, pp. 280–298.
- [9] V. Ozceyhan, S. Gunes, O. Buyukalaca, N. Altuntop, Heat transfer enhancement in a tube using circular cross sectional rings separated from wall, *Appl. Energy*, Vol. 85, 2008, pp. 988–100.
- [10] P. Promvong, S. Sripattanapipat, W. Jedsadaratanachai, Numerical simulation of Al₂O₃-water nanofluid flow and heat transfer in a tube with angled rings, *Adv. Mater. Res.* Vol. 931–932, 2014, pp. 1168–1172.
- [11] S. Sripattanapipat, S. Tamna, N. Jayranaiwachira, P. Promvong, Numerical heat transfer investigation in a heat exchanger tube with hexagonal conical-ring inserts, *Energy Procedia* , Vol. 100, 2016, pp. 522 – 525.